AIAA 81-4212

Contamination Effect of MMH/N_2O_4 Rocket Plume Product Deposit

Chang-Keng Liu* and A.P.M. Glassford†
Lockheed Palo Alto Research Laboratories, Palo Alto, Calif.

The predominant species in the plume residue resulting from the incomplete combustion of MMH and N_2O_4 during the pulse mode operation of the bipropellant motors has been found to be monomethylhydrazine nitrate (MMH-HNO_3). At orbital altitude, it is also the most detrimental condensible matter as other species in the plume product or unburned propellant droplets have vapor pressures too high to be of concern. Quantitative data on contamination effects from the MMH/N_2O_4 thrusters in pulse mode operations are limited. This paper reports experiments in which several types of thermal control surfaces were systematically contaminated with a range of amounts of synthesized MMH-HNO_3, after which the resulting change in solar absorptance was measured. Limited experiments were also made to measure the change of solar transmittance of fused silica disks.

Introduction

DURING pulse-mode operation of the bipropellant attitude-control rocket motors the high chamber temperatures required for complete combustion of the fuels cannot be attained. This is particularly true in short duration pulse width operations (10 ms-15 ms) with the engine cold. The products of complete combustion are usually highly volatile gases while some of the products of incomplete combustion are frequently condensible at near-ambient temperatures. Hence, if the thruster plume impinges upon thermal control surfaces, the products of incomplete combustion may condense and degrade the optical performance of the surfaces.

In general, the products of incomplete combustion of nitrogen tetroxide (N_2O_4) and amine fuels are nitrates. This paper considers the contamination effects produced on 25°C thermal control surfaces by monomethylhydrazine nitrate (MMH-HNO_3), which is the principal product of incomplete combustion of N_2O_4 and MMH(CH_3NHNH_2) condensible at this temperature. MMH-HNO_3 has been positively identified by analysis of residues left at 25°C on the walls of simulation chambers after MMH/N_2O_4 thruster test firings.[1,2] It is highly hygroscopic and is usually found in the form of clear, amber, or even brown liquid droplets.[3] Spectrographic analysis reveals that these different colored liquids are all forms of MMH-HNO_3, with the coloration being due probably to impurities. For the purpose of making systematic contamination effects studies, it is more convenient to use MMH-HNO_3 synthesized in the laboratory. Spectrographic analysis of the synthesized material reveals it to be essentially identical to that produced by an actual thruster. In fact, synthesized samples have been found to acquire a similar yellow coloration in the laboratory environment. (It is noted that these conclusions are based upon laboratory simulations. For condensing surfaces at temperatures other than 25°C, MMH-HNO_3 may not be the principal condensible contaminant. In real applications engine type, duty cycle, location in the plume, and the space environment may also affect contaminant type.)

The magnitude of the plume contamination problem can be assessed at the design stage, either by simulation testing or by analytical studies. Many tests have been reported in which thermal control materials and solar cells have been placed at various locations in the plume of thrusters under test in simulation chambers.[4-11] Prefiring and postfiring measurements of their optical properties give reliable data on the contamination threat on surfaces in specific locations relative to the thruster, and for specific firing schedules. However, such tests are expensive and yield data strictly applicable only to specific situations. A less costly and more flexible approach is to perform analytical studies. Such studies require data relating the amount of contaminant on a surface to the resulting change in properties.

To the authors' knowledge the only published data of this general type are Refs. 3, 12, and 13, which describe a recent and relatively comprehensive series of experiments to measure thruster plume mass flow, deposit thickness, change of properties of optical materials, and degradation of solar cells using an N_2O_4/monomethylhydrazine motor. However, the experiments relating deposit thickness to change in transmittance were made for wavelengths in the infrared region for deposits on a 20 K germanium surface. At this temperature MMH-HNO_3 is a minor component of the deposit. The solar cell degradation was recorded as a function of exposure time, not deposit thickness. The authors know of no published data relating change of thermal control surface propertis to deposit thickness at 25°C, which is a representative spacecraft surface temperature. To fill this need some experiments have been conducted in which several types of thermal control surfaces were systematically contaminated with a range of amounts of synthesized MMH-HNO_3, after which the resulting change in solar absorptance was measured. Limited experiments were also made to measure the change of solar transmittance of fused silica disks. Because of the inherent difficulties encountered in working with MMH-HNO_3, the experimental techniques used were ncessarily less rigorous than would have been desired. The reported data are intended to serve as an indication of trends until data from more sophisticated simulations become available.

The Contaminant

Preparation of MMH-HNO_3

The sample of MMH-HNO_3 was prepared in the laboratory by the treatment of MMH with equimolar solution of dilute nitric acid and the removal of water under reduced pressure.[2] A typical solution was prepared by placing 1.000 g of MMH in a 3-necked round bottom flask equipped with an external ice bath and teflon magnetic stirrer. 10.0 g of ice were weighed and added to the MMH. Then 11.3 ml of 1.91*N* nitric acid

Received Sept. 30, 1980; revision received March 3, 1981.

*Staff Scientist, Materials Sciences Laboratory.
†Staff Scientist, Materials Sciences Laboratory. Member AIAA.

were added dropwise from a buret, with stirring. The temperature of the flask was maintained below 12°C due to the hypergolic nature of MMH. Stirring was continued for 5 min. The solution was then filtered through a sintered glass filter to remove dust, etc., and then poured into a graduated cylinder. Its volume was found to be 21.5 ml. The weight of the nitric acid was given by $1.91 \times 63 \times 11.3/1000 = 1360$ g. The amount of MMH-HNO_3 salt in unit volume of the solution was then 0.110 g/cm^3.

The solution was clear when first prepared, and remained so for the first portion of the test program. At later stages it acquired a yellowish color. During the tests, MMH-HNO_3 samples were obtained from the dark yellow liquid deposit on a front surface aluminum mirror, the light yellow liquid deposits on an Al/OSR and on a S-13G white paint surface. The infrared spectra of these MMH-HNO_3 samples were obtained by a Perkin-Elmer Model 621 Grating Infrared Spectrophotometer over the wavelength range of 2.5 to 30.30 μm. The results were compared to the infrared spectrum of N_2O_4-MMH combustion residue given by Refs. 3, 7, and 14, and the infrared spectrum of residue from synthesis of MMH-HNO_3 and of pulse-generated contaminants given by Ref. 2. It was found that the spectra from each of the MMH-HNO_3 samples were the same and excluding the differences in sample thickness, the spectra obtained from the three samples compare nearly "peak for peak" with the published spectra.

Evaporation Characteristics of MMH-HNO_3

The rate of evaporation was measured in a Thermal Analysis Apparatus (TAA). Detailed description of the TAA is given in Ref. 15. The MMH-HNO_3 aqueous solution was placed in the TAA sample holder. The bell jar was first evacuated to pressure of 20 Pa, and then filled with helium to nearly 1 atm. The liquid nitrogen pot was filled and the entire apparatus cooled rapidly. During this time evaporation of the MMH-HNO_3 solution was inhibited by the helium gas pressure. When the sample pot had cooled to about −70°C the bell jar was re-evacuated. Pressures below 10^{-4} Pa were then readily attained since at −70°C and below the evaporation rate of the MMH-HNO_3 is negligible. The procedure from this point on was to heat the sample pot slowly and collect the evaporating molecular flux from the sample pot on the cold quartz crystal microbalance (QCM) collector. When a sufficiently large deposit had been collected the sample pot was allowed to recool, after which the QCM was slowly heated until all of the deposit had been evaporated. The QCM was then recooled and the cycle of sample heating with QCM collection followed by QCM warmup was repeated. This cycle was repeated a number of times until the original specimen of MMH-HNO_3 in the sample pot had been completely evaporated.

In the test about 5 or 6 cycles of sample pot warmup followed by QCM warmup were made before all the samples had been evaporated from the pot. Data in the first two QCM warmups indicated that the deposits had been water. The third QCM warmup produced an evaporation characteristic displaced to slightly higher temperatures than the H_2O characteristic. It is believed that the main species in the third warmup is H_2O, with the perturbation being produced by carried-over MMH-HNO_3. In the first two sample pot heatings the pot temperature did not exceed −38°C. The third heating raised the sample pot temperature to about 20°C before an adequate QCM deposit was obtained. It is felt that the temperature step from −38°C to 20°C is large enough that, were there another species with evaporation characteristics close to that of water, it would have shown up unambiguously. As it is, this temperature jump brought the pot temperature very close to the regime in which MMH-HNO_3 began to evaporate, giving support to the carry-over theory.

In the fourth and subsequent cycles it was necessary to heat the sample pot to the 30°C to 60°C range to get a significant deposit on the QCM. It was presumed that at this time all of the H_2O had been driven from the sample material and that the collected species was pure MMH-HNO_3. Using geometric relationships the evaporation rate from the pot can be inferred.[15] These data are shown in Fig. 1. The rate of evaporation can be approximated by $\dot{m}_e = 2.28 \times 10^8 \exp(-H/RT)$ g/cm^2 s, where $H = 20{,}480$ cal/g mol, R is the gas constant, and T is in K.

Test Procedure

Approach

The test approach was to deposit synthesized MMH-HNO_3 solution onto a range of thermal control surface samples and measure the surface property. The amount of solution deposited was varied so that the relationship between deposit mass per unit area and resulting change in surface properties could be determined systematically. It is not known whether, in practical situations in the space environment, MMH-HNO_3 deposits exist as liquid or solid deposits. It was therefore intended to perform tests with deposits in the form of both liquid solution and crystalline solid. Difficulty was often experienced in removing the water completely from the liquid solution, and it was not possible to obtain solid MMH-HNO_3 in all cases. However, since water absorbs only weakly in the stronger portion of the solar spectrum, its presence was not expected to influence significantly the magnitude of the contamination effect produced by a given amount of MMH-HNO_3.

The surface properties were measured in the clean state using a Cary-Model 14 spectrophotometer, which measures the diffuse spectral reflectance (R_λ) and the transmittance (T_λ) in the range of 0.27 to 1.8 μm with a maximum uncertainty of ±0.005 reflectance unit. The solar reflectance is calculated by integrating the spectral reflectance with respect to the solar spectral irradiance. The solar absorptance (α_s) is then calculated by subtracting the solar reflectance from unity. The solar transmittance is calculated in a similar manner when the apparatus is run in the transmittance mode.

Contamination of Test Surfaces

By use of a micropipette, the neutral solution was deposited with various calculated amounts onto a number of test sample surfaces. Since it was desired to measure the contamination effect of both the liquid solution and the solid MMH-HNO_3, two sets of surface samples were contaminated for each surface type. The mass of MMH-HNO_3 on the test surfaces per unit area was found from the known volume of the liquid

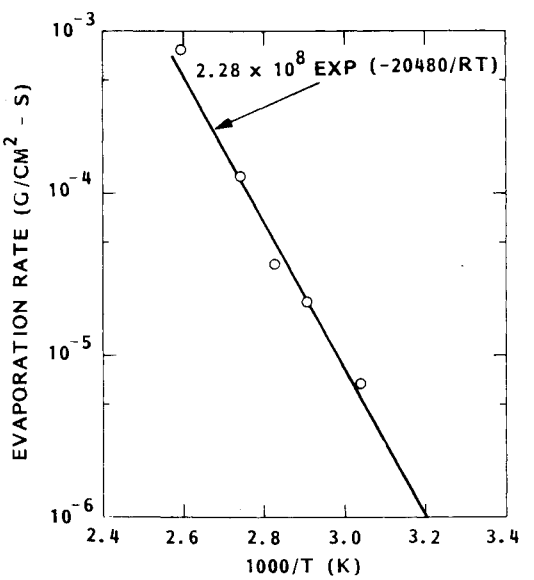

Fig. 1 Estimated evaporation rate of MMH-HNO_3.

deposit, the measured base area of the deposit, and the MMH-HNO_3 concentration of 0.11 g/cm^3, determined earlier. One set of surfaces was then placed in vacuum dessicators for removal of water under reduced pressure. The removal of water from the MMH-HNO_3 solution deposited was not wholly successful and the deposits remained in a light brown liquid droplet form on some of the test surfaces. Three earlier samples, one with solid and two with liquid deposit, were transferred from the vacuum dessicator to a bell jar system. The system was first cryopumped to 2×10^{-5} Pa for 24 h and then at room temperature and 4.3×10^{-5} Pa for 96 h. No visual change was observed on any of the deposits. The liquid droplets remained in liquid form and the solid deposit did not seem to decrease in size. In the subsequent surface property change measurements no substantial difference was found between the data for MMH-HNO_3 in aqueous solution or as a solid. The need to improve the efficiency of water removal therefore appeared to be a relatively minor issue.

After contamination of the test surfaces their properties were again measured. Surfaces with solid clear crystal deposit had to be measured in an inert gas environment as the MMH-HNO_3 salt is extremely hygroscopic. Since the deposits were originally made in droplet form, they were generally smaller in base area than the spectrophotometer beam, which varied from approximately 0.64×1.91 cm in the ultraviolet to 0.16×1.27 cm in the near infrared region. Thus, only a portion of the beam was incident upon the MMH deposit, the remainder striking the uncontaminated area around the deposit. Because of its integrative capability the spectrophotometer combines the reflected beams from these two regions and indicates the average reflectance over the beam area. If the absorption by the deposit were proportional to thickness of deposit then the average loss of reflectance produced by a deposit of given mass and density would be the same, whether the deposit were concentrated in one region of the beam or were uniformly distributed over its area. In this case, the change in reflectance measured by the spectrophotometer may be associated with a deposit mass per unit area equal to the deposit total mass divided by the geometric beam area. For small deposits the error should be small.

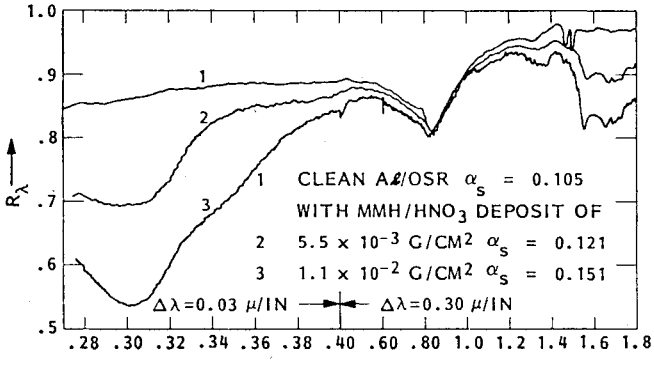

Fig. 2 Spectral reflectance of MMH-HNO_3 liquid deposit on Al/OSR.

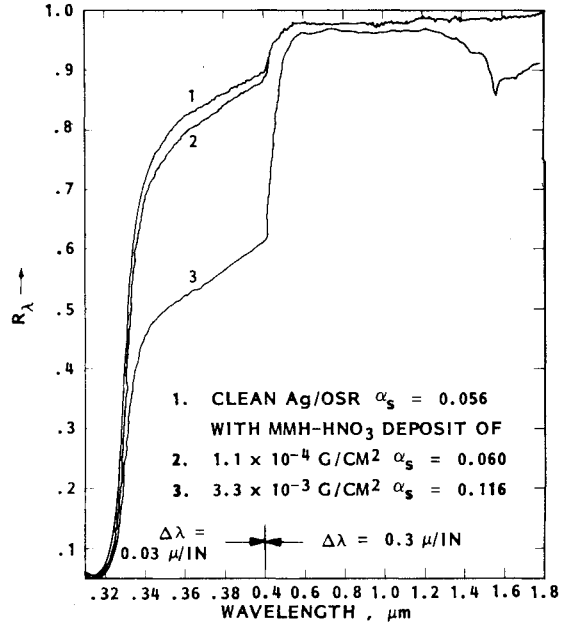

Fig.3 Spectral reflectance of MMH-HNO_3 liquid deposit on Ag/OSR.

Ultraviolet Exposure

After measurement of the properties of these contaminated surfaces, one Al/OSR and two Al/FOSR surfaces were exposed to ultraviolet radiation in vacuum at a level of 2 suns for 325 ESH (equivalent sun hours defined as intensity multiplied by exposure time). The object of this limited test was to obtain a qualitative indication of the effect of ultraviolet radiation on contaminated surfaces, so that the

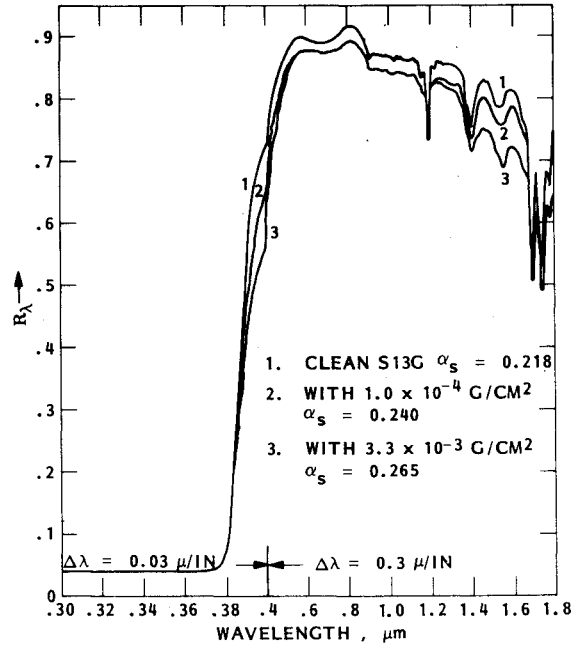

Fig. 4 Spectral reflectance of MMH-HNO_3 liquid deposit on S-13G white coatings.

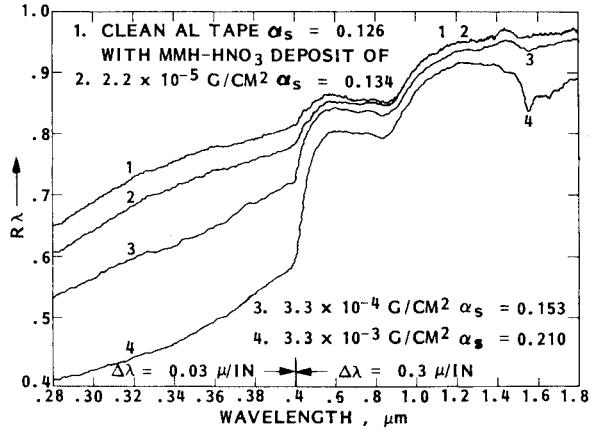

Fig. 5 Spectral reflectance of MMH-HNO_3 liquid deposit on Al tape.

need for more comprehensive, systematic tests could be determined. During this exposure most of the deposit disappeared, and the remaining deposit was no longer hygroscopic, indicating a chemically different species. Following the exposure, the solar absorptance of these surfaces was again measured.

Test Results and Discussions

Changes of surface properties due to MMH-HNO_3 liquid deposits are given in Figs. 2-9, that of solid deposits in Figs. 10-12. Due to limit in space, the spectral reflectance data of liquid deposit on flexible aluminized and silverized FEP Teflon (Al/FOSR and Ag/FOSR) as well as that of solid deposit on Ag/FOSR and Al-tape are not included. However, a summary of test results on solar absorptance and transmittance changes are given in Table 1 and Figs. 8, 9, and 12. The effects due to the deposits as well as subsequent uv exposure are discussed below.

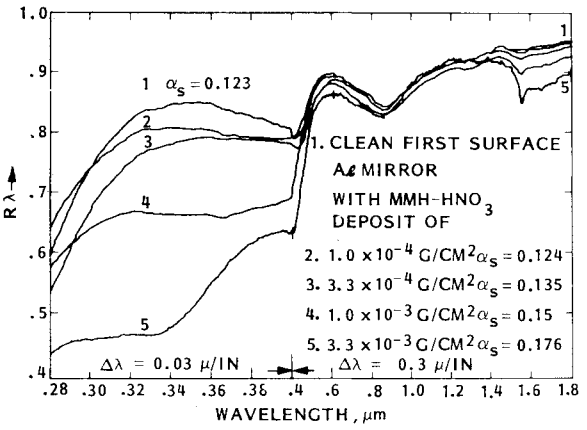

Fig. 6 Spectral reflectance of MMH-HNO_3 liquid deposit on Al mirror.

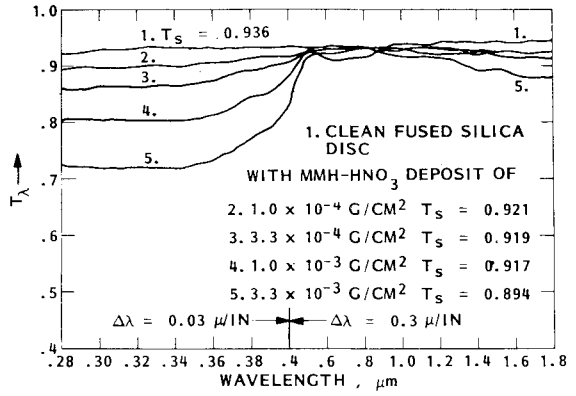

Fig. 7 Spectral transmittance of MMH-HNO_3 liquid deposit on fused silica.

Liquid Deposit

Figure 2-6 show the spectral reflectance of various surfaces both clean and with various amounts of liquid contaminants. Figure 7 shows the spectral transmittance of clean and contaminated fused silica disks. It can be seen that MMH-HNO_3 absorbs most strongly below about 0.4 μm. There is also another noticeable but less marked region of absorption

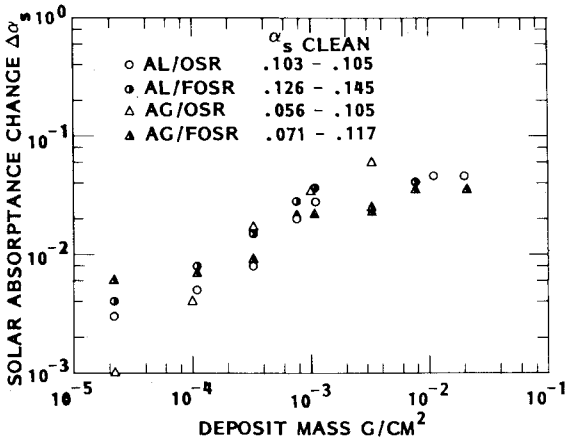

Fig. 8 Solar absorptance of MMH-HNO_3 liquid deposit on optical solar reflectors.

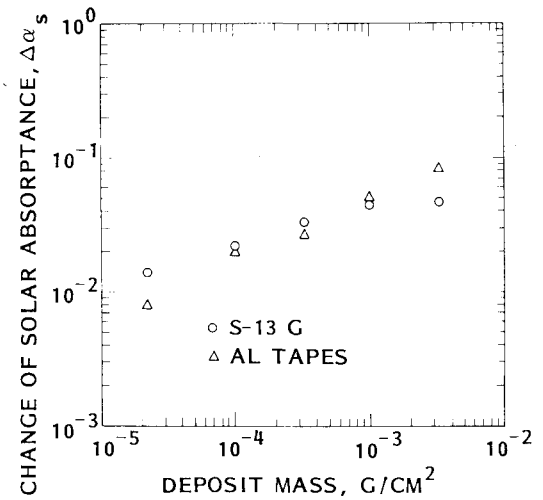

Fig. 9 Solar absorptance of MMH-HNO_3 liquid deposit on Al tapes and S-13G white coatings.

Table 1 Contamination effect of MMH-HNO_3 deposit

Test surface	Solid deposit: No. of deposit	Solid deposit: Mass (g/cm^2)	Solid deposit: $\Delta\alpha_s$	Liquid deposit: No. of deposit	Liquid deposit: Mass (g/cm^2)	Liquid deposit: $\Delta\alpha_s$ ($-\Delta T_s$)
Al/OSR[a]	1	0.028	0.087	10	2.2×10^{-5}-2×10^{-2}	0.002-0.046
Ag/OSR[a]				5	2.2×10^{-5}-3.3×10^{-3}	0.001-0.06
Al/FOSR[b]	3	$2.1\text{-}3.5\times10^{-2}$	0.063-0.187	8	2.2×10^{-5}-7.7×10^{-3}	0.004-0.041
Ag/FOSR[c]	4	0.014-0.035	0.055-0.108	8	2.2×10^{-5}-2.2×10^{-2}	0.006-0.035
S-13G				5	2.2×10^{-5}-3.3×10^{-3}	0.014-0.047
Al-tape[d]	8	2.8×10^{-4}-2.8×10^{-2}	0.005-0.115	5	2.2×10^{-5}-3.3×10^{-3}	0.008-0.084
Al-mirror				4	1×10^{-4}-3.3×10^{-3}	0.124-0.176
Fused silica		0.063-0.187		4	1×10^{-4}-3.3×10^{-3}	(0.015-0.042)

[a] Aluminized and silverized second face mirror with an 8-mil-thick quartz front. [b] Flexible aluminized FEP Teflon. [c] 5-mil FEP Teflon/Ag/Inc./SR-585. [d] 2-mil dead soft aluminum 3003-0 alloy backing with 2-mil pressure-sensitive acrylic adhesive on one side of backing.

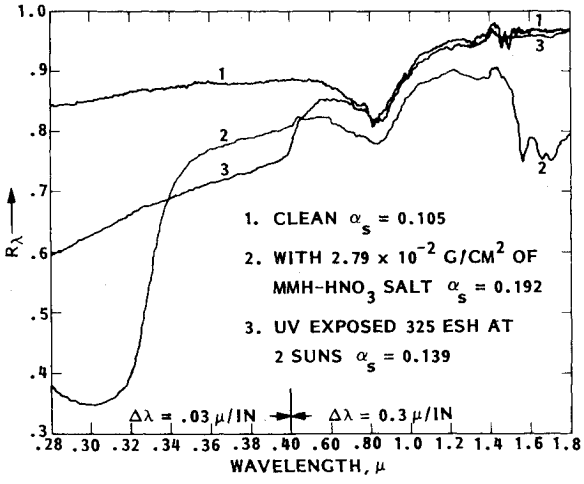

Fig. 10 Spectral reflectance of MMH-HNO$_3$ salt on Al/OSR with uv exposure.

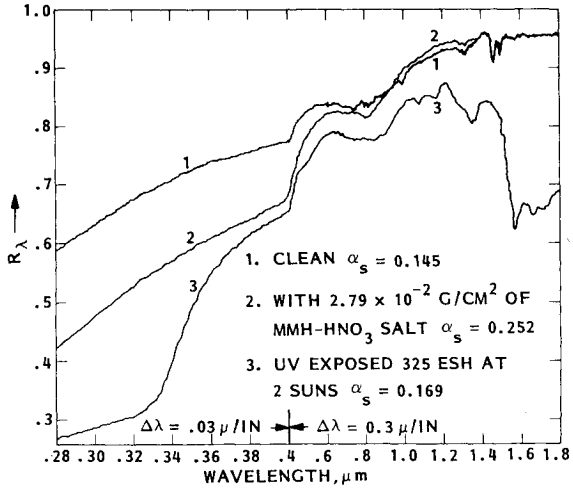

Fig. 11 Spectral reflectance of MMH-HNO$_3$ salt on Al/FOSR with uv exposure.

above about 1.2 μm. The degree to which the absorption spectrum is changed varies from surface to surface, depending on the spectrum of the clean surface. The effect of MMH-HNO$_3$ on absorption below 0.4 μm is least for S13G, for which the clean surface has a cutoff below 0.4 μm. On other surfaces, it is seen that increase in absorption begins in the uv and visible region with low density but occurs only with higher density in the range above 0.4 μm. Figures 8 and 9 show the change of solar absorptance as a function of MMH-HNO$_3$ deposit mass per unit area. Because the solar spectrum is relatively less intense below 0.4 μm, the noted differences below 0.4 μm in the spectral absorption changes for different surfaces have a reduced influence on solar absorptance. Hence all surfaces have generally similar net changes as apparent in Figs. 8 and 9.

Solid Deposit

The spectral absorptances of the surfaces with solid deposits of MMH-HNO$_3$ were similar to those obtained for surfaces with liquid solution deposits. As an example, the spectral reflectance of clean and contaminated Al/OSR samples as shown by curves 1 and 2 in Fig. 10 are comparable to curves 1 and 3 in Fig. 2. The similarity is expected since water is present to some degree in the solid as well as the liquid, as water of crystallization, and it does not absorb strongly in the spectral range measured.

Figure 12 shows the relationship between the change in solar absorptance and the solid deposit density for the four

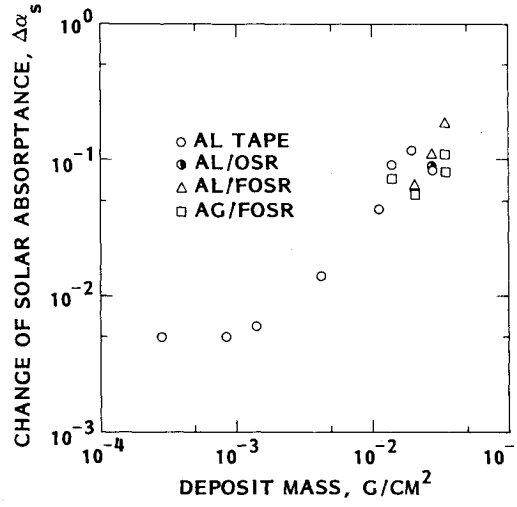

Fig. 12 Solar absorptance of MMH-HNO$_3$ salt on thermal control surfaces.

Table 2 Effect of ultraviolet radiation[a]

Material	Al/FOSR	Al/FOSR	Al/OSR
Clean α_s	0.145	0.145	0.105
MMH-HNO$_3$ deposit, g/cm^2	2.09×10^{-2}	2.79×10^{-2}	2.79×10^{-2}
$\Delta\alpha_s$ before irradiation	0.063	0.107	0.087
$\Delta\alpha_s$ after irradiation	0.020	0.024	0.034

[a] Irradiation level: 2 suns, 325 equivalent sun hours.

materials tested. Most of the data points are for relatively high mass densities and trends are less obvious than they are for the liquid deposit data. However, there is good agreement in magnitude of $\Delta\alpha_s$ between the solid and liquid data, which would be expected because of the low absorptance of water in the intense portion of the solar spectrum. The Al tape $\Delta\alpha_s$ data for low average solid deposit densities lie below the values obtained for the liquid deposit. The liquid data are probably more reliable than the solid data, since with the liquid deposit a more even distribution of MMH-HNO$_3$ is obtained. During attempts to remove water by evacuation, disturbance of the droplets due to sudden boiling was observed. This might cause ejection of an amount of MMH-HNO$_3$, making the final true deposit mass less than calculated from the original liquid volume and concentration. Allowance for possible lost mass would bring the solid data for Al tape closer to the liquid data. Finally, the Al tape data for liquid deposit are more regular, suggesting a lower degree of random error.

Effect of Ultraviolet Exposition

Figures 10 and 11 show the spectral reflectance of an Al/OSR and an Al/FOSR specimen while clean, contaminated, and subsequently exposed to ultraviolet radiation. It was noted earlier that after irradiation the deposit seemed to be smaller so the mass density is uncertain. Also, the deposit appeared to be no longer hygroscopic. Significant differences are evident for the contaminated surfaces before and after exposure. The reflectance spectrum given by curves 3 in Figs. 10 and 11 show good recovery of spectral reflectance at wavelength longer than 0.5 μm. At wavelength shorter than 0.34 μm the values of spectral reflectance have also increased but are still below that of a clean Al/OSR surface. The differences in the form of the spectral reflectance and loss of hygroscopity suggest that a chemical change could have

occurred during irradiation. Unfortunately, further investigation of any possible chemical changes was outside the scope of the program. The spectral reflectance data for the other Al/FOSR and the Al/OSR surfaces shared qualitatively similar characteristics. The data from the three tests are summarized in Table 2.

The effect of space radiation on matter has been discussed by Green and Hamman[16] on spacecraft materials in general and by Broadway[17] on thermal control coatings, in particular. However, the effects of combined exposure to contaminant deposit and orbital solar radiation are not well known. Recent flight data of a thermal control coatings experiment on the Air Force Space Test Program STP P72-1 satellite has become available.[18] The change in solar absorptance was measured during 5 yr of space exposure (10,866 equivalent sun hours). The data showed that the Ag/OSR was the most stable material during the 5-yr exposure. The Al/FOSR was also quite stable with a total increase in solar absorptance of about 0.08. The degradation was believed to be caused by the contamination from the outgassing materials on the satellite. It is not clear whether contamination can also be caused from any thruster plumes. Still, it is of interest to note that present data (Figs. 10 and 11) of solar absorptance change after 325 ESH fall within the range of the flight data of Al/FOSR between initial and 3 months (543 ESH) in space. (See Ref. 18, p. 26.)

Conclusion

An assessment on the exhaust plume characteristics of a MMH/N_2O_4 thruster has been made. It is concluded that the potentially deleterious effects may result for certain space system configurations since significant contaminant influx and deposition may take place. The evaporation characteristics of the plume product, MMH-HNO_3, were investigated. The rate of evaporation can be approximated by $2.28 \times 10^8 \exp(-20{,}480/RT)$ g/cm^{2}s.

The change of surface property due to the MMH-HNO_3 deposit on various thermal control surfaces and optical surfaces was measured and the results have been presented. The results indicated that the salt deposit is highly hygroscopic but stable in vacuum at room temperatures; solar absorptance of thermal control surfaces measured ex situ generally increases with deposit mass; after uv irradiation, the deposit loses mass and is no longer hygroscopic and reflectance recovers significantly in the near i.r. and partly in the uv; degradation on spectral transmittance of fused silica is greatest in the uv region and significant in the near i.r. region at larger deposit mass.

It should be noted that the conclusions obtained from the data in the present test apply only to the specific set of experimental conditions under which the contaminant deposit, solid or liquid, was made as well as the manner in which the measurements were made. The contaminant as observed ex situ exists as clear, transparent,[5] or dark brown[7] liquid droplets due to its hygroscopic characteristics. During the in situ measurements conducted later,[6,9] the deposit was not visible to the observer. It is really not known which form (liquid droplet or solid deposit) is the actual state of the contaminant as it exists on the contaminated surfaces in orbital conditions. The best way is to collect test data on deposit in both solid and liquid droplet forms.

It is recommended that additional tests should be conducted on candidate spacecraft thermal control and optical surface samples and possible synergism between the MMH-HNO_3 deposit and uv irradiation be investigated. Also, the uv-exposed deposit should be analyzed for possible chemical changes. The results could be most useful in prediction of contaminant buildup and estimate of subsequent degradation of thermal control surfaces.

Acknowledgments

This work was performed by Lockheed Palo Alto Research Laboratory in support of LMSC Space System Division, U.S. Air Force and NASA Program Offices, and as part of a Lockheed Independent Research Program. The MMH-HNO_3 solution was prepared by Dr. John A. Gallaghan of Dept. 85-51 at the LMSC Santa Cruz Facility. The i.r. spectra of the MMH-HNO_3 samples were obtained by G. McCauley of Dept. 52-35.

References

[1] Etheridge, F.G. and Boudreaux, R.A., "Attitude-Control Rocket Exhaust Plume Effect on Spacecraft Functional Surfaces," *Journal of Spacecraft and Rockets,* Vol. 7, Jan. 1970, pp. 44-48.

[2] Takimoto, H.H. and Denault, G.D., "Rocket Plume (N_2O_4/MMH) Impingement on Aluminum Surface," *Journal of Spacecraft and Rockets,* Vol. 7, Nov. 1970, pp. 1372-1374.

[3] Alt, R.E., "Bipropellant Engine Plume Contamination Program," Vol. 1, ARO Inc., AEDC-TR-79-28, Dec. 1979.

[4] Cassidy, J.F., "Space Simulation Experiments on Reaction Control Systems Thruster Plumes," AIAA Paper 72-1071, 1972.

[5] Jack, J.R., Spisz, E.W., and Cassidy, J.F., "The Effect of Rocket Plume Contamination on the Optical Properties of Transmittance and Reflecting Materials," AIAA Paper 72-56, 1972.

[6] Sommers, R.D., Raquet, C.A., and Cassidy, J.F., "Optical Properties of Thermal Control Coatings Contaminated by a MMH/N_2O_4 5-Pound Thruster in a Vacuum Environment with Solar Simulation," See also Progress in Astronautics and Aeronautics Series, "Thermal Control and Radiation" Vol. 31, edited by Chang-Lin Tien, MIT Press, Cambridge, Mass., 1973, pp. 145-158.

[7] Spisz, E.W., Bowman, R.L., and Jack, J.R., "Exhaust Plume and Contamination Characteristics of a Bipropellant (MMH/N_2O_4) RCS Thruster," 7th JANNAF Plume Technology Conference, Redstone Arsenal, Ala., April 1973, NASA TMX-68212, 1972.

[8] Bowman, R.L., Spisz, E.W., and Jack, J.R., "Effect of Contamination on the Optical Properties of Transmitting and Reflecting Materials Exposed to MMH/N_2O_4 Rocket Exhaust," 7th JANNAF Plume Technology Conference, Redstone Arsenal, Ala., April 1973, NASA RMX-68204, 1973.

[9] Sommers, R.D. and Raquet, C.A., "Effect of Thruster Pulse Length Thruster-Exhaust Damage of S-13G White Thermal Control Coatings," 7th JANNAF Plume Technology Conference, Redstone Arsenal, Ala., April 1973, NASA TMX-68213, 1973.

[10] Spisz, E.W., Bowman, R.L., and Jack, J.R., "Plume Mass Flow and Damage Distributions for an MMH/N_2O_4 RCS Thruster," paper presented at 7th AIAA/ASTM/IES Space Simulation Conference, Los Angeles, Calif., Nov. 1973, NASA TMX-71465, 1973.

[11] Bowman, R.L., Spisz, E.W., Sommers, R.D., and Jack, J.R., "Skylab Plume Contamination Effects," paper presented at the 7th AIAA/ASTM/IES Space Simulation Conference, Los Angeles, Calif., Nov. 1973, NASA TMX-71474, 1973.

[12] Powell, H.M., Price, L.L., and Alt, R.E., "Bipropellant Engine Plume Contamination Porgram," Vol. II, ARO Inc., AEDC-TR-79-28, Nov. 1979.

[13] Palmer, K.F., Wood, B.E., and Roux, J.A., "Infrared Optical Properties of Solid Mixtures of Molecular Species at 20°K," AEDC-TR-80-30, Jan. 1981.

[14] Roux, J.A., Wood, B.E., Pipes, J.G., and Smith, A.M., "Optical Properties of Cryo-contaminants," Presented at USAF/NASA International Spacecraft Contamination Conference, USAF Academy, March 1978.

[15] Liu, C.K. and Glassford, A.P.M., "Kinetic Data for Diffusion of Outgassing Species from RTV 560 Silicone Rubber," *Journal of Vacuum Science and Technology,* Vol. 15, No. 5, Sept./Oct. 1978, pp. 1761-1768.

[16] Green, M.L. and Hamman, D.J., "Radiation Effects Design Handbook, Section 5. The Radiations in Space and Their Interactions with Matter," NASA CR-1871, Sept. 1971.

[17] Broadway, N.J., "Radiation Effects Design Handbook, Section 2. Thermal-Control Coatings," NASA CR-1786, June 1971.

[18] Winn, R.A., "ML-101 Thermal Control Coatings: Five Year Space Exposure," AFML-TR-78-99, July 1978.